Technobius, 2025, 5(3), 0087, DOI: https://doi.org/10.54355/tbus/5.3.2025.0087

Technobius
https://technobius.kz/

e-ISSN
2789-7338

Article

Eco-efficient composite cements and arbolite using burnt clay shale from the Mynaral deposit

Baurzhan Amiraliyev[1], Kuanysh Imanaliyev[1,*], Zhambul Aymenov[1], Erzhan Kuldeyev[2], Bakhrom Tulaganov[3]

[1]M. Auezov South Kazakhstan University, Shymkent, Kazakhstan
[2]K.I. Satpayev Kazakh National Research Technical University, Almaty, Kazakhstan
[3]Tashkent University of Architecture and Civil Engineering, Tashkent, Uzbekistan
*Correspondence: kuanish.69@mail.ru

Abstract. This study investigates the potential of burnt clay shale (BCS) from the Mynaral deposit (Zhambyl region, Kazakhstan) as an active mineral additive in composite cements and arbolite. Thermal and X-ray diffraction analyses revealed progressive dehydration, decarbonation, and decomposition of kaolinite, chlorite, and calcite, with optimal activation at 900 °C. Pozzolanic activity tests confirmed maximum reactivity at this temperature. Mechanical testing showed that 10–15% BCS increased cement strength up to 51 MPa, while higher dosages reduced performance. Arbolite samples with ash-and-slag binders and controlled alkaline additives demonstrated superior density and strength, supported by SEM evidence of dense crystalline microstructures and strong binder–filler adhesion. The findings highlight BCS as an effective, eco-friendly component reducing clinker consumption and CO_2 emissions.
Keywords: arbolite, rice husks, strength, binders, composite cement, active mineral additives, clay shale.

1. Introduction

Today, the construction industry actively uses local raw materials and industrial waste to produce building materials. In this regard, the production of arbolite, a material known for over a century, is considered one of the most profitable and effective ways to recycle wood waste [1]. Arbolite is a type of lightweight concrete that uses organic components, primarily wood chips, as its filler. This makes it environmentally friendly and safe for health. The wood chips also act as a reinforcing element, providing arbolite with high bending strength. This property is superior to that of aerated concrete and cement stone. Due to this feature, additional reinforcement of walls is not required when constructing buildings made of arbolite [2].

According to [3], due to its high content of wood components, arbolite is prone to moisture absorption. To protect it from getting wet, it is necessary to either plaster or cover the exterior walls. However, it also dries quickly. Another disadvantage is the uneven surface of the blocks. Unlike aerated concrete, the porous structure of arbolite leads to a disruption in its ideal geometric shape during production. [4] considered the use of geopolymer foam concrete, a material that is expensive and difficult to produce. At the same time, [2] suggest using hemp as a thermal insulation material, which can lead to a number of problems. One of the priority areas in this area is the development and improvement of the technology for the production of arbolite, which is an effective type of lightweight concrete. It is a typical local building material. Arbolite production is based on the use of waste from logging, sawmilling, woodworking, etc. [5].

The availability of local raw materials in each region allows for the development of arbolite production for local construction needs. Wood is a scarce material in Kazakhstan, and agricultural

waste can be used as a filler for arbolite. Research and development work [3] conducted to study arbolite and improve its production technology has shown the potential for using local agricultural waste in arbolite production. Given the above, the use of rice husks as a raw material for the production of arbolite blocks appears relevant when combining them with a composite cement as a binding agent for these blocks. Such a cement should contain active mineral additives that help reduce carbon dioxide emissions during production.

Cement plants are allocated significantly larger quotas compared to gypsum and silicate plants. This is due to following reasons: firstly, cement plants are usually large, with output of up to 1.2 million tons per year; secondly, when firing the raw material mixture, consisting of 70-75% limestone, a significant amount of CO_2 is released according to the reaction $CaCO_3 \rightarrow CaO + CO_2$; thirdly, when firing cement clinker using the dry method, 100-120 kg of conventional fuel is consumed per 1 ton of clinker and, accordingly, carbon is oxidized to dioxide and CO_2 is released a lot [6]. This suggests the existence of environmental problems in cement production, and due attention should be paid to solving them; cement plants should switch to "green" technologies that do not pollute the environment with various harmful emissions. One way to make cement production more environmentally friendly is the incorporation of a mineral additive – clay shales, which are rocks of metamorphic origin [7], [8].

The active mineral additives studied in [7], [8] may allow partial replacement of the clinker component in cement grinding, which will increase production efficiency, produce environmentally friendly products, reduce flue gas emissions into the atmosphere, fill the deficit of building materials in the country, reduce its cost, and increase the export potential of the Republic. Although studied works offer important directions for decarbonization, they are limited in the detailed analysis of practical barriers, focusing on conceptual or managerial aspects, ignoring the specific engineering, economic, and technical difficulties in implementing such solutions in real production. In this regard, this study aims at improving the arbolite production technology by incorporating rice husk as a filler and burnt clay shale as an active mineral additive for a composite cement.

2. Methods

The study was carried out using three main raw materials: clay shale from the Mynaral deposit (Zhambyl region, Kazakhstan), Portland cement (PC) clinker obtained from the Sastobe cement plant (Shymkent, Kazakhstan), and natural gypsum stone from a local deposit. Representative samples were collected, quartered to obtain averaged specimens, and homogenized. The shale was preliminarily ground to pass through a No. 008 sieve to ensure uniformity. Chemical analysis of all three materials was performed by X-ray fluorescence (XRF) spectrometry [9] using a PANalytical Axiosm spectrometer (Almelo, The Netherlands), which provided the quantitative oxide composition required for subsequent evaluations.

The clay shale was further examined by differential thermal analysis (DTA) [10] on a Q-1500 derivatograph (Budapest, Hungary) in the temperature range of 20-1000 °C at a heating rate of 10 °C/min. Along with the DTA curve, thermogravimetric (TG) and differential thermogravimetric (DTG) curves were recorded to identify dehydration, dehydroxylation, and decarbonization processes characteristic of the mineral phases present.

After thermal analysis, the shale was fired in an electric furnace SNOL 7.2/1100 (SnolTherm, Narkūnai, Lithuania) at three different temperatures, 700, 800, and 900 °C, with an isothermal holding period of 20 minutes. The mineralogical transformations occurring during firing were studied using X-ray diffraction (XRD) [11] analysis on a Bruker AXS D8 (Bruker Corporation, Karlsruhe, Germany) diffractometer equipped with a Cu Kα source and Vantec PSD detector, scanning across a 2θ range of 6-70°. Phase identification was carried out with reference to the ICDD PDF database.

The pozzolanic activity of the fired shale was then determined by the classical lime absorption method [12], [13]. One gram of finely ground shale was placed into 100 mL of saturated

lime solution with a CaO concentration of 1.05-1.15 g/L. The mixture was shaken and titrated with 0.05 N HCl every two to three days over 30 days using methyl orange as an indicator. The activity was expressed as the amount of $Ca(OH)_2$ absorbed per gram of additive, which provided a quantitative measure of the reactivity of the fired material.

To evaluate the effect of shale additives on cement performance, six composite cement (CC) compositions were prepared by co-grinding clinker, gypsum (5 wt.%), and shale fired at three temperatures (700, 800, and 900 °C) in proportions ranging from 5 to 30 wt.% (Table 1). A reference cement composed of 95% clinker and 5% gypsum was also produced.

Table 1 – Composition of the studied CCs, %

Composition No.	Clinker	Gypsum	Burnt clay shale (BCS)		
			700 °C	800 °C	900 °C
Reference	95	5	-	-	-
1	90	5	5	5	5
2	85	5	10	10	10
3	80	5	15	15	15
4	75	5	20	20	20
5	70	5	25	25	25
6	65	5	30	30	30

The compressive strength of prism samples with dimensions of 40×40×160 mm was determined after 28 days of curing according to [14] and [15] standards, using a PGM-100MG4 press (Stroipribor, Chelyabinsk, Russia) at a loading rate of 2 MPa/s.

Based on the obtained composite cements, five compositions of arbolite were manufactured with rice husk as the organic filler (Table 2).

Table 3 – Composition of the studied arbolite samples, %

No.	Alumosilicate component		An aqueous solution of an alkaline component		
	Ash and slag	CC	Liquid glass	Chromepik	Alkali
1	89.25	-	8.8	1.95	-
2	90.2	-	5.9	3.9	-
3	90.77	-	5.9	-	3.33
4	92.2	-	-	7.8	-
5	96	5	-	4.0	-
6	91.5	5	-		3.5

Cube specimens of 100×100×100 mm in size were molded and subjected to heat-moisture treatment in a steaming chamber KUP-1 (RosPribor, Belgorod, Russia) at 70 °C, following an isothermal curing cycle of 3+3+8+3 hours to accelerate strength gain. The true density of arbolite was measured using the Le Chatelier flask [16] and compressive strength was determined after 60 hours of curing in accordance with [17].

Finally, to study the internal structure of the produced composites, microphotographs of fractured arbolite samples were obtained by scanning electron microscopy (SEM) [18]. A Zeiss LEO Supra 35 microscope operating at 20 kV. The ×1000 and ×10000 magnifications were used to examine the morphology of hydration products, the adhesion of cementitious binder to the rice husk particles, and the overall development of the microstructure that defines the performance of the arbolite.

3. Results and Discussion

Table 2 below shows the results of XRF spectrometry that revealed the chemical composition of the raw materials for the composite cement.

Table 1 – Averaged chemical composition of raw materials, wt.%

Material	Calcination losses	SiO_2	$A1_2O_3$	Fe_2O_3	CaO	MgO	SO_3	Other
PC clinker	0.31	18.56	3.27	3.06	55.09	1.52	5.55	5.04
Clay shale	-	70.41	10.38	3.73	5.38	0.75	0.03	9.32
Gypsum stone	20.30	2.80	0.49	traces	30.98	traces	42.80	2.63

The XRF analysis shows that Portland cement clinker is dominated by calcium oxide (55.09%), with significant contributions from silicon dioxide (18.56%) and alumina (3.27%), which are typical of clinker phases. The clay shale is characterized by a very high silica content (70.41%) combined with alumina (10.38%) and minor amounts of iron oxide (3.73%) and calcium oxide (5.38%). This composition indicates that the shale can act as a siliceous-aluminous component in cement blends. The gypsum stone exhibits a high loss on calcination (20.30%) due to its water content and is mainly composed of calcium oxide (30.98%) and sulfur trioxide (42.80%), which are characteristic of gypsum ($CaSO_4 \cdot 2H_2O$). Only trace amounts of Fe_2O_3 and MgO were detected. This confirms its role as a sulfate carrier for controlling cement setting.

Figure 1 below shows the results of the DTA of the clay shale.

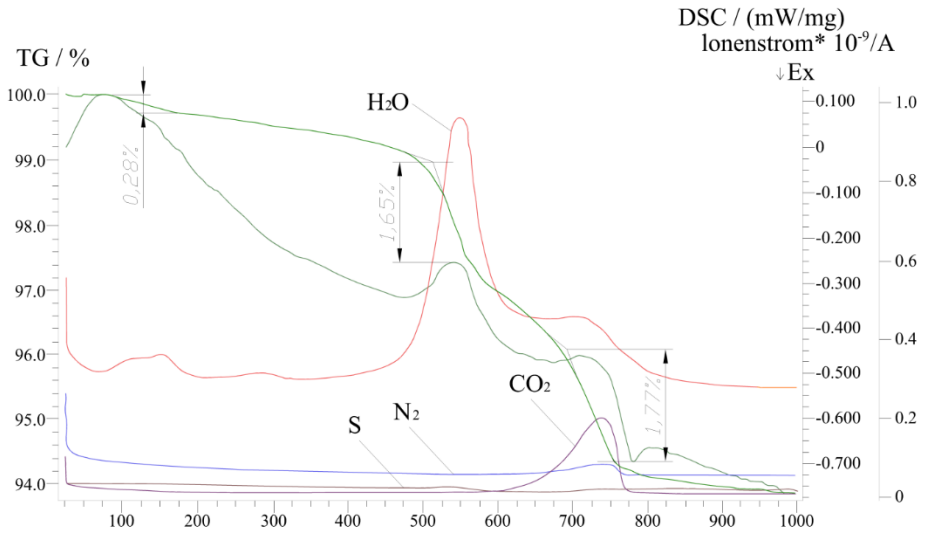

Figure 1 – Thermogram of clay shale

The thermogram of clay shale demonstrates three distinct intervals of mass loss and associated thermal effects. In the temperature range of 80-170 °C, a mass loss of about 0.28% is observed, corresponding to the removal of physically bound water from clay minerals such as beidellite, halloysite, montmorillonite, and dickite. Between 530-568 °C, the second stage of dehydration occurs, resulting in a 1.65% mass loss attributed to the release of physicochemically bound water remaining in the same group of minerals. At higher temperatures, in the 700-760 °C range, a further 1.77% mass reduction is recorded, which corresponds to the loss of chemically bound crystalline water from hydroaluminosilicate minerals, including kaolinite, halloysite, and donbassite. The differential thermal and thermogravimetric curves show endothermic peaks indicating the intensity of these processes. The peak near 130 °C reflects the initial removal of absorbed moisture, which becomes most pronounced at 570 °C. A subsequent peak at 710–730 °C indicates the onset of decarbonization of calcium carbonate (calcite). Differential thermal analysis further confirms these processes, with moisture loss identified at 530–568 °C and decarbonization of calcite at around 780 °C, both accompanied by endothermic reactions. In addition, the curves show evidence of gas release, including sulfur (S), nitrogen (N_2), and carbon dioxide (CO_2), at elevated temperatures. These results are consistent with previous studies, which have shown that clay shales undergo stepwise dehydration and decarbonation processes during heating, leading to

the formation of reactive aluminosilicate phases. For instance, [19] reported that the removal of bound water from clay minerals and the decomposition of calcite above 700 °C significantly increases the pozzolanic reactivity of calcined clays.

Figure 2 below shows the results of the XRD of the fired clay shale.

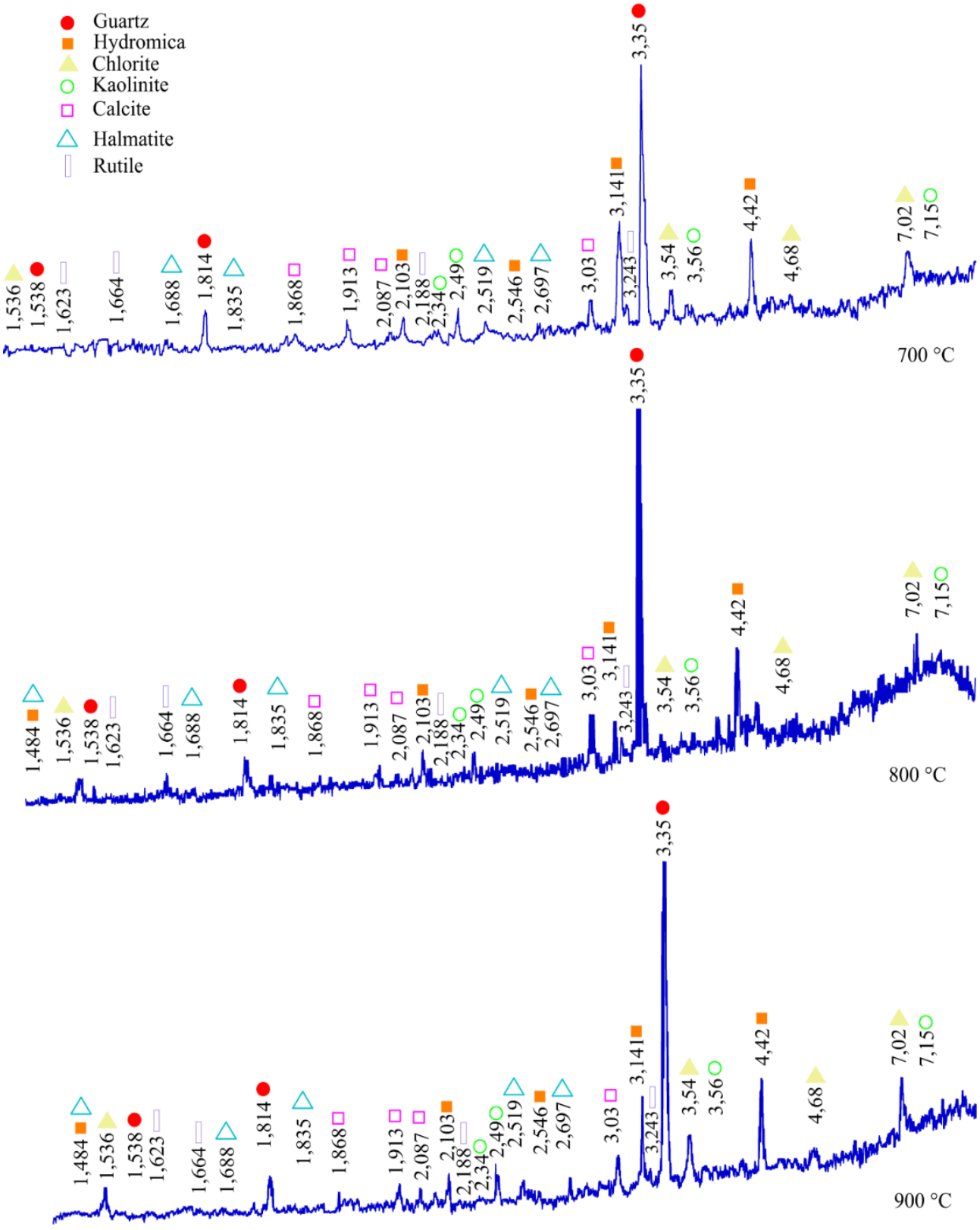

Figure 2 – XRD of fired clay shale

The X-ray diffraction patterns of clay shale fired at 700, 800, and 900 °C show significant mineralogical changes. At all three firing temperatures, the dominant reflections correspond to quartz (SiO_2) with a characteristic maximum at d = 3.35 Å. Alongside quartz, peaks of hydromica, chlorite, kaolinite, calcite, hematite, and rutile are identified. At 700 °C, reflections of kaolinite (d = 7.15, 3.56, 2.30 Å) and chlorite (d = 7.02, 4.68, 2.69 Å) remain well pronounced, indicating incomplete dehydroxylation of layered aluminosilicates. Calcite peaks (d = 3.03, 1.913, 2.087 Å) are also visible, suggesting partial retention of carbonate phases. At 800 °C, the intensity of kaolinite and chlorite reflections decreases, showing progressive breakdown of these minerals. Calcite peaks are still observed, but with reduced intensity, indicating the onset of decarbonization. Quartz reflections remain stable, while hematite and rutile are also detected. At 900 °C, kaolinite reflections almost disappear, confirming its decomposition, while quartz becomes the most stable phase. Chlorite peaks are further weakened, and calcite reflections diminish sharply, reflecting active decarbonization of carbonate minerals. The persistence of quartz and hematite at this temperature highlights their thermal stability under firing. Overall, the XRD analysis confirms that increasing firing temperature results in the gradual decomposition of clay minerals (kaolinite, chlorite, hydromica) and carbonates, with quartz remaining stable throughout, and new crystalline phases such as hematite contributing to the formation of reactive structures that enhance pozzolanic activity.

Figure 3 presents the results of pozzolanic activity tests of clay shale determined by the lime absorption method.

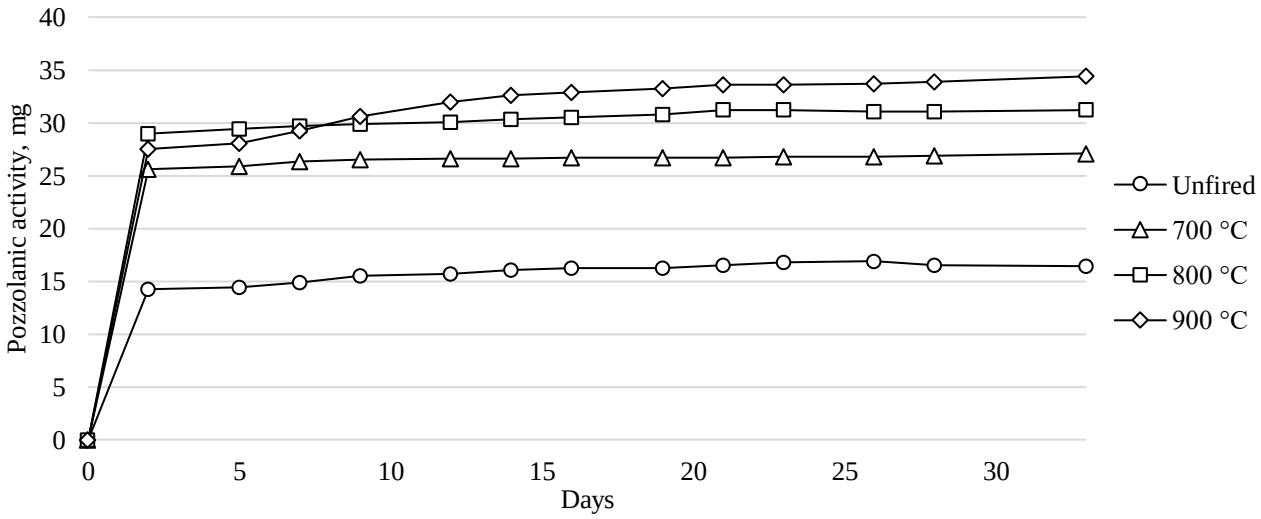

Figure 3 – Dependence of clay shale pozzolanic activity on firing temperature

The pozzolanic activity of the clay shale varies significantly depending on the firing temperature. The unfired shale shows the lowest activity, reaching only 15-18 mg of $Ca(OH)_2$ absorbed per gram of additive after 30 days. Shale fired at 700 °C exhibits moderate activity, stabilizing at about 25-27 mg. Increasing the firing temperature to 800 °C results in higher reactivity, with values rising to 30–32 mg by day 30. The maximum pozzolanic activity is observed in shale fired at 900 °C, where absorption reaches approximately 34-35 mg, demonstrating the highest lime-binding capacity. In all cases, a sharp increase in activity occurs within the first 2-3 days, followed by a gradual stabilization over the 30-day observation period. The results confirm that firing temperature plays a decisive role in enhancing the reactivity of clay shale, with optimal activity achieved at 900 °C. These findings are consistent with previous research showing that calcination significantly enhances the pozzolanic activity of clays and shales. [20] observed that thermal activation of illitic and kaolinitic clays at 900 °C leads to maximum lime consumption and improved pozzolanic performance. The observed rapid initial uptake of $Ca(OH)_2$ followed by stabilization aligns with the kinetics of pozzolanic reactions reported in these studies.

Figure 4 presents the results of compressive strength tests of composite cements with different contents of fired clay shale at 700, 800, and 900 °C.

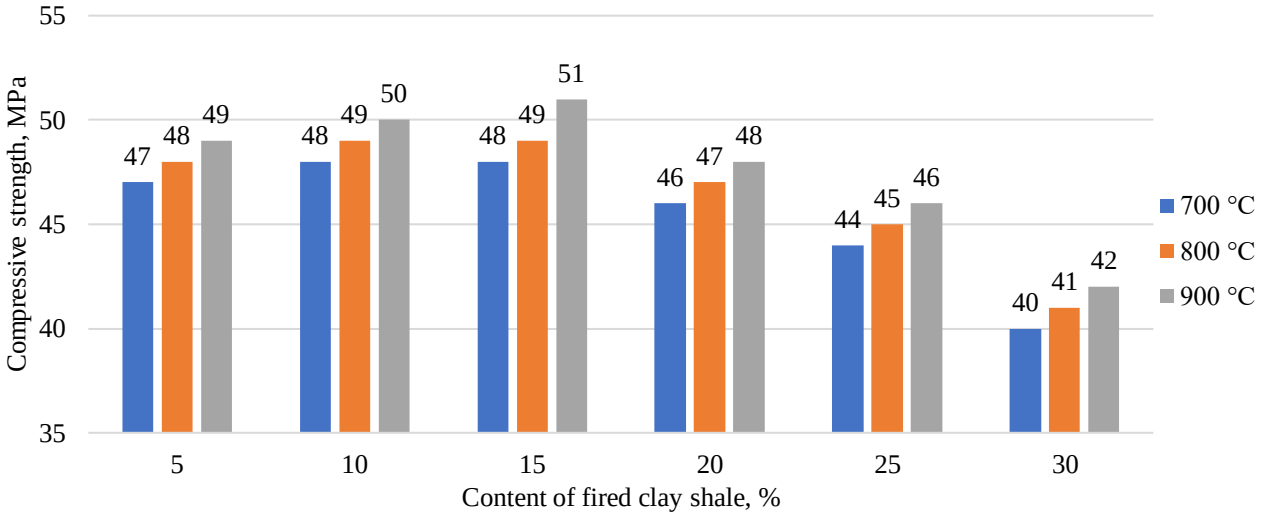

Figure 4 – Dependence of the compressive strength of the composite cement on the content and firing temperature of clay shale

The control sample without additives showed a compressive strength of 49 MPa after 28 days. When fired shale was introduced, the strength increased at additive levels of 5-15%. At 5% content, compressive strength rose slightly to 47-49 MPa depending on firing temperature. At 10% content, the values increased further to 48-50 MPa. The maximum compressive strength of 51 MPa was obtained with 15% shale fired at 900 °C, confirming this as the optimal dosage for strength gain. Beyond this level, a gradual decrease in strength was observed. At 20% content, compressive strength fell to 46-48 MPa, while at 25% it dropped further to 44-46 MPa. At the highest replacement level of 30%, strength decreased markedly to 40-42 MPa. These results indicate that while small additions of fired clay shale (up to 15%) enhance the compressive strength of composite cement, higher proportions reduce it, regardless of firing temperature. Similarly, [21] observed that optimal replacement levels of calcined clays generally lie between 10–15%, beyond which compressive strength decreases.

Figure 5 shows the results of density and compressive strength tests of arbolite samples.

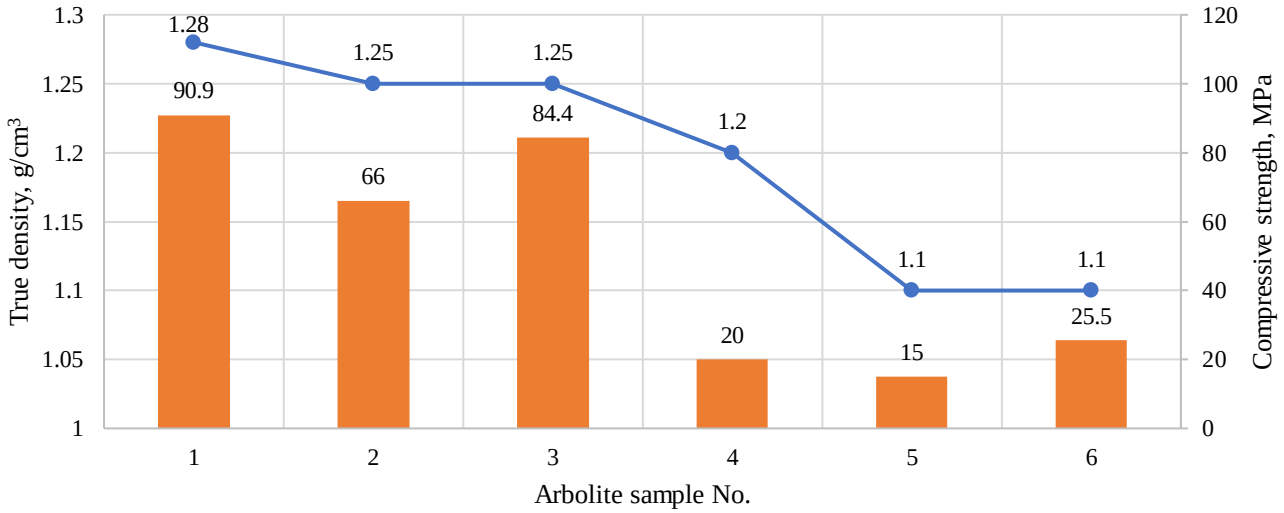

Figure 5 – True density and compressive strength of arbolite

The data show that samples 1-3, which used ash and slag as the main aluminosilicate component together with liquid glass and small amounts of chromepik or alkali, achieved relatively

high compressive strengths of 90.9, 66, and 84.4 MPa, with true densities of 1.25-1.28 g/cm^3. In contrast, samples 4–6, where ash and slag were combined with larger amounts of chromepik or alkali and, in two cases, 5% composite cement, displayed much lower compressive strengths of 20, 15, and 25.5 MPa, with true density reduced to 1.1-1.2 g/cm^3. These results indicate that the binder composition has a critical influence on arbolite properties: mixtures with ash and slag and liquid glass promote higher strength and density, while increasing the share of chromepik, alkali, or composite cement reduces these values markedly.

Figure 6 shows the results of SEM of the fractured arbolite based on composite cement using a clay shale.

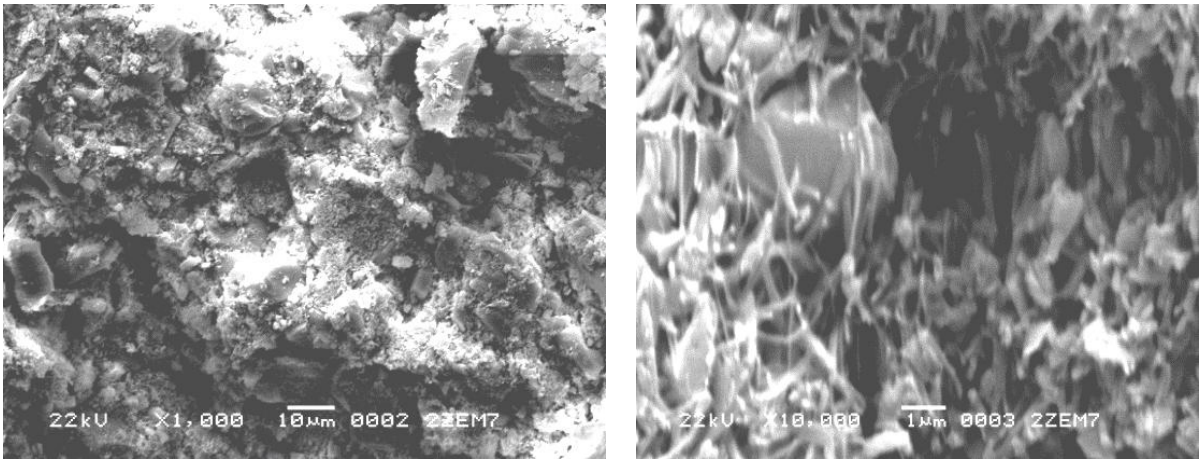

a) ×1000 b) ×10000

Figure 6 – Microphotographs of fractured arbolite

The micrographs demonstrate the formation of a crystalline microstructure within the cement matrix, which serves as a framework for the material. The images confirm that hydration products are well distributed and that the structure formation process begins at the initial stages of hardening. The photographs clearly illustrate the adhesion of the binder to the organic filler, showing close contact between the cement matrix and rice husk particles. The introduction of composite cement with active mineral additives modifies the structure of arbolite, accelerating the appearance and aggregation of new formations in the microcrystalline system. The results highlight that, compared to control compositions, arbolite with composite cements develops a denser and more stable microstructure, which directly influences its strength and durability. Similar findings were presented by [22], who demonstrated that active mineral additions foster the early formation of hydration products, resulting in a more compact and durable microstructure. Future work should focus on long-term durability studies of arbolite with burnt clay shale additives under varying environmental conditions to confirm their practical performance.

4. Conclusions

The study revealed clear patterns in the behavior of clay shale and its effect on composite binders. Thermal analysis and XRD showed that structural transformations of kaolinite, chlorite, and calcite at firing temperatures up to 900 °C are directly linked to the rise in pozzolanic activity, confirming 900 °C as the optimal activation point. A consistent trend was observed in mechanical tests: moderate additions of burnt shale (10-15%) improved cement strength, whereas higher dosages reduced it due to dilution effects. In arbolite, compositions with ash-and-slag binders and controlled alkaline additives provided the best balance of density and strength, while excessive chromepik, alkali, or cement reduced performance. Microstructural analysis confirmed that these patterns result from the formation of a denser crystalline framework and improved binder-filler adhesion. Altogether, the results demonstrate that optimized use of burnt clay shale can enhance composite cements and arbolite while reducing clinker demand and environmental impact.

Acknowledgments

This research was funded by the Science Committee of the Ministry of Science and Higher Education of the Republic of Kazakhstan (Grant No. BR21882292 – "Integrated development of sustainable construction industries: innovative technologies, optimization of production, effective use of resources and creation of technological park").

References

[1] M. Dlimi, R. Agounoun, I. Kadiri, R. Saadani, and M. Rahmoune, "Thermal performance assessment of double hollow brick walls filled with hemp concrete insulation material through computational fluid dynamics analysis and dynamic thermal simulations," *e-Prime - Advances in Electrical Engineering, Electronics and Energy*, vol. 3, p. 100124, Mar. 2023, doi: 10.1016/j.prime.2023.100124.

[2] B. Martínez, V. Mendizabal, M. B. Roncero, E. Bernat-Maso, and L. Gil, "Towards sustainable building solutions: Development of hemp shiv-based green insulation material," *Constr Build Mater*, vol. 414, p. 134987, Feb. 2024, doi: 10.1016/j.conbuildmat.2024.134987.

[3] K. Imanaliyev, B. Amiraliyev, K. Akmalaiuly, E. Kuldeyev, E. Yunusaliyev, and Z. Aymenov, "Research of technological parameters for producing thermal insulating arbolite based on developed slag alkali binders," *Technobius*, vol. 4, no. 3, p. 0065, Sep. 2024, doi: 10.54355/tbus/4.3.2024.0065.

[4] X. Ding, J. Yu, J. Lin, Z. Chen, and J. Li, "Experimental investigations of prefabricated lightweight self-insulating foamed concrete wall panels," *Structures*, vol. 61, p. 106001, Mar. 2024, doi: 10.1016/j.istruc.2024.106001.

[5] I. E. Kazimagomedov, L. V Trykoz, F. I. Kazimagomedov, and A. V Rachkovskiy, "Study of the forming processes of the arbolite structure during the chemical activation of flax shove," *IOP Conf Ser Mater Sci Eng*, vol. 708, no. 1, p. 012086, Dec. 2019, doi: 10.1088/1757-899X/708/1/012086.

[6] N. N. Zhanikulov *et al.*, "Receiving Portland Cement from Technogenic Raw Materials of South Kazakhstan," *Eurasian Chemico-Technological Journal*, vol. 21, no. 4, pp. 333–340, Dec. 2019, doi: 10.18321/ectj890.

[7] B. Isakulov, A. Issakulov, and A. Dąbska, "Structure Formation and Curing Stage of Arbolite–Concrete Composites Based on Iron-Sulfur Binders," *Infrastructures (Basel)*, vol. 10, no. 7, p. 179, Jul. 2025, doi: 10.3390/infrastructures10070179.

[8] B. Amiraliyev *et al.*, "Heat Treatment of Clay Shales and Their Utilization as Active Mineral Additives for the Production of Composite Cements," *Journal of Composites Science*, vol. 9, no. 6, p. 269, May 2025, doi: 10.3390/jcs9060269.

[9] *ISO 12677:2011 Chemical analysis of refractory products by X-ray fluorescence (XRF) — Fused cast-bead method*. 2011, p. 75.

[10] *ISO 11357-1:2023 Plastics — Differential scanning calorimetry (DSC)*. 2023, p. 34.

[11] D. Alderton, "X-Ray Diffraction (XRD)," in *Encyclopedia of Geology*, Elsevier, 2021, pp. 520–531. doi: 10.1016/B978-0-08-102908-4.00178-8.

[12] I. V. R. Ramanujam, K. R. Reddy, and N. V. Ramana, "Evaluation of Pozzolanic activity and lime reactivity of fly ash, GGBS, mica powder and pumice as binders," *E3S Web of Conferences*, vol. 529, p. 01008, May 2024, doi: 10.1051/e3sconf/202452901008.

[13] H. Wang, X. Liu, and Z. Zhang, "Pozzolanic activity evaluation methods of solid waste: A review," *J Clean Prod*, vol. 402, p. 136783, May 2023, doi: 10.1016/j.jclepro.2023.136783.

[14] *GOST 310.4-81 Cements. Methods of bending and compression strength determination*. 1981, p. 11.

[15] *GOST 30744-2001 Methods of testing with using polyfraction standard sand*. 2001, p. 36.

[16] *ASTM C188-17 Test Method for Density of Hydraulic Cement*. ASTM International, 2017, p. 3. doi: 10.1520/C0188-17.

[17] *GOST 10180-2012. Concrete. Methods for Determining Strength Using Control Specimens*. Moscow, Russia, 2018, p. 36.

[18] *ISO/TS 21383:2021 Microbeam analysis — Scanning electron microscopy — Qualification of the scanning electron microscope for quantitative measurements*. 2021, p. 59.

[19] E. Güneyisi, M. Gesoğlu, Özturan T., and K. Mermerdaş, "Comparing Pozzolanic Activity of Metakaolin and Calcined Kaolin, and Their Effects on Strength of Concrete," in *10th International Congress on Advances in Civil Engineering (ACE 2012)*, Ankara, Turkey : Middle East Technical University, 2012, pp. 1–10.

[20] A. Tironi, M. A. Trezza, A. N. Scian, and E. F. Irassar, "Assessment of pozzolanic activity of different calcined clays," *Cem Concr Compos*, vol. 37, no. 1, 2013, doi: 10.1016/j.cemconcomp.2013.01.002.

[21] J. Ambroise, M. Murat, and J. Péra, "Hydration reaction and hardening of calcined clays and related minerals V. Extension of the research and general conclusions," *Cem Concr Res*, vol. 15, no. 2, 1985, doi: 10.1016/0008-8846(85)90037-7.

[22] R. Walker and S. Pavía, "Physical properties and reactivity of pozzolans, and their influence on the properties of lime-pozzolan pastes," *Materials and Structures/Materiaux et Constructions*, vol. 44, no. 6, 2011, doi: 10.1617/s11527-010-9689-2.

Information about authors:
Baurzhan Amiraliyev – PhD Student, Department of Silicate Technology and Metallurgy, M. Auezov South Kazakhstan University, Shymkent, Kazakhstan, badam777@inbox.ru
Kuanysh Imanaliyev – Candidate of Technical Sciences, Associate Professor, Head of the Department of Architecture and Urban Planning, M. Auezov South Kazakhstan University, Shymkent, Kazakhstan, kuanish.69@mail.ru
Zhambul Aymenov – Doctor of Technical Sciences, Professor, Director of the Research Institute of Natural and Technical Sciences, M. Auezov South Kazakhstan University, Shymkent, Kazakhstan, zhambul_ukgu@mail.ru
Erzhan Kuldeyev – Candidate of Geological and Mineralogical Sciences, Professor, Vice-Rector for Science and Corporate Development, K.I. Satpayev Kazakh National Research Technical University, Almaty, Kazakhstan, e.kuldeyev@satbayev.university
Bakhrom Tulaganov – PhD, Rector, Tashkent University of Architecture and Civil Engineering, Tashkent, Uzbekistan, bahrombek@gmail.com

Author Contributions:
Baurzhan Amiraliyev – data collection, testing, concept, methodology.
Kuanysh Imanaliyev – concept, resources, supervision, analysis.
Zhambul Aymenov – funding acquisition, drafting, editing.
Erzhan Kuldeyev – resources, drafting, editing.
Bakhrom Tulaganov – analysis, visualization, data processing.

Conflict of Interest: The authors declare no conflict of interest.

Use of Artificial Intelligence (AI): The authors declare that AI was not used.

Received: 13.05.2025
Revised: 20.09.2025
Accepted: 28.09.2025
Published: 29.09.2025